Normal stresses in elastic networks

Normal stresses in elastic networks

Adrian R. Cioroianu and Cornelis Storm
Department of Applied Physics and Institute for Complex Molecular Systems, Eindhoven University of Technology, P. O. Box 513, NL-5600 MB Eindhoven, The Netherlands

(Received 4 June 2013; revised manuscript received 11 September 2013; published 4 November 2013)

When loaded in simple shear deformation, polymeric materials may develop so-called *normal stresses*: stresses perpendicular to the direction of the applied shear. These normal stresses are intrinsically nonlinear: basic symmetry considerations dictate they may only enter at $O(\gamma^2)$, with γ the dimensionless shear strain. There is no fundamental restriction on their sign, and normal stresses may be positive (pushing outward) or negative (pulling inward). Most materials tend to dilate in the normal direction, but a wide variety of biopolymer networks including fibrin and actin gels have been reported to present anomalously large, *negative* normal stresses—a feature which has been ascribed to the intrinsic elastic nonlinearity of semiflexible fibers. In this work, we present analytical results on a model nonlinear network, which we expand to the required nonlinear order to show that due to geometric, rather than elastic, nonlinearities (negative) normal stresses *generically* arise in filamentous networks—even in networks composed of linear, Hookean springs. We investigate analytically and numerically how the subsequent addition of elastic nonlinearities, nonaffine deformations, and filament persistence through cross-linkers augment this basic behavior.

DOI: 10.1103/PhysRevE.88.052601 PACS number(s): 61.41.+e, 83.10.−y, 87.16.Ka, 83.60.Df

I. INTRODUCTION AND SUMMARY

The world, natural as well as man-made, abounds with materials composed of interlinked filamentous units. The cytoskeleton, the extracellular matrix, cartilage, but also rubbers and plastics owe their mechanical properties predominantly to networks of large aspect ratio polymers which, in many cases, are joined together by cross-links. This general motif allows for significant stiffness, strength, and resilience—even in lightweight, open geometries, and even in the presence of significant disorder, and thus represents a particularly economical and robust design principle for soft materials, biological and synthetic.

Their abundance in nature, combined with the possibility of precision mechanical manipulation of single molecules, has spurred a renewed interest in the structure-property relationships for these filamentous materials: how the mechanical properties relate to the microscopic structure. While this interest previously focused predominantly on explaining or understanding emergent mechanical properties given a certain microscopic structure, the insights its questions have provided is increasingly put to use to purposely target specific mechanical properties in designer (soft) materials or metamaterials, obtained by directing the spatial arrangement of fibers, by manipulating the mechanical properties of fibers, or by the addition of active, nonequilibrium components.

Many of these efforts are, in one form or another, bioinspired: the properties of self-assembled biological materials offer unique functionality and the ability to copy (some of) them in synthetic or reconstituted matter would open up interesting new opportunities for industrial and medical materials.

Many of these sought-after mechanical properties involve the nonlinear regime of elastic response. The tendency to strain stiffen [1–4], for instance, has been well documented and researched in biological gels and tissues, and has been observed in similarly constituted gels of both reconstituted proteinaceous fibers and synthetic polymers [5–7]. In this article, we focus on another striking nonlinear feature of biopolymer gels: negative normal stresses. When deformed in shear, these gels exhibit inward normal thrusts, strongly pulling inward on the upper and lower surfaces. While negative normal stresses are the exception, rather than the rule, in soft materials (foams [8] and sphere packings [9] exhibit positive normal stresses) the effect has been reported in a wide variety of systems, including liquid crystalline polymers [10], suspensions [4,11,12], emulsions [13], marginal solids [9], clays [14], some granular systems [15], and carbon nanotubes, both single walled [16] and multiwalled [17,18]. Moreover, negative normal stresses are a promising feature for the creation of mechanical metamaterials, along with other unusual mechanical response such as negative compressibility [19] and negative Poisson's ratios [20,21].

Here, however, we focus on semiflexible (bio)polymer gels, where negative normal stresses were recently reported to feature generically and very prominently [22]. For this class of systems the effect was ascribed to the typical asymmetry in the force-distance curve of semiflexible polymers [23,24], which strongly resist extension but remain relatively soft in compression. Indeed, buckling of a significant fraction of the constituent polymers was shown to occur in numerical and analytical work. In this paper, we argue that such buckling need not be the only explanation for negative normal stresses and that, indeed, the effect is even more generic. In addition to elastic nonlinearities of the filaments, geometric nonlinearities of the network as a whole also very naturally give rise to negative normal stresses. We demonstrate this analytically for affinely deforming systems, but show, numerically, that the effects survive when nonaffine deformations are allowed. Our work complements earlier work by Janmey and others, but presents a crucial extension to the theory by expanding to the requisite nonlinear order all important contributions, geometrical and elastic, for an analytically tractable polymer model that allows one to disentangle the effects of both. For stiffer semiflexible networks, we find that indeed the elastic

nonlinearity dominates, but very soon—when the persistence length ℓ_p becomes of the order of the contour length ℓ_c—geometric and elastic nonlinearities acquire similar magnitudes. Our work provides a more complete understanding of the different effects at play in the normal stress response of network materials, allowing for more precise control over these properties in synthetic designer materials.

Our paper is organized as follows. In Sec. II, we review the requisite concepts from finite-strain elasticity theory which we need to compute stresses from strains beyond linear response. Section III relates these concepts to discrete spring networks and derives a general expression for the Cauchy stress tensor for affinely deforming networks. In Sec. IV, we apply the formalism to a simple nonlinear elastic model that allows one to obtain analytical expressions for shear and normal stresses and disentangles geometric and elastic nonlinearities. In Sec. V, we present numerical simulations for the Mikado model [25] to assess if and how shear and normal stresses are augmented in the presence of nonaffine deformations. Section VI presents some general considerations regarding the role of nonaffinity and the relevance of affine reference deformations. In Sec. VII we summarize our findings and present some conclusions.

II. STRESSES AND STRAINS: GENERAL FRAMEWORK

A general deformation $\mathbf{R}$ maps points $\mathbf{x}$ in a reference space onto their images $\mathbf{x}'$ in a target space as

$$\mathbf{x} \mapsto \mathbf{x}'(\mathbf{x}) = \mathbf{R}(\mathbf{x}). \tag{1}$$

There is no deformation when $\mathbf{R}(\mathbf{x}) = \mathbf{x}$. To distinguish nontrivial deformations, we split off the *displacement vector* $\mathbf{u}$:

$$\mathbf{R}(\mathbf{x}) = \mathbf{x} + \mathbf{u}(\mathbf{x}). \tag{2}$$

Assuming that distortions vary slowly in space, we may linearize this around the origin $\mathbf{O}$ to find

$$R_i(\mathbf{x}) \approx R_i(\mathbf{O}) + \left(\frac{\partial R_i(\mathbf{x})}{\partial x_j}\right) x_j. \tag{3}$$

In what follows, we will subtract any uniform translations (i.e., $\mathbf{R}(\mathbf{O}) = \mathbf{O}$), and summation over repeated indices will be implied. The first derivatives appearing in this equation define the deformation tensor $\Lambda(\mathbf{x})$,

$$\Lambda_{ij}(\mathbf{x}) = \frac{\partial R_i(\mathbf{x})}{\partial x_j} = \delta_{ij} + \frac{\partial u_i}{\partial x_j} \equiv \delta_{ij} + \eta_{ij}. \tag{4}$$

The tensor η is called the displacement gradient tensor. A transformation is called *affine* when the deformation tensor is constant throughout the the entire body or volume that is deformed. In other words, the deformation is affine if and only if $\Lambda \neq \Lambda(\mathbf{x})$. If this is the case, the constant deformation tensor Λ effects a true linear mapping

$$\mathbf{x} \mapsto \mathbf{x}' = \Lambda \cdot \mathbf{x}. \tag{5}$$

While affinely deforming systems are rarely, if ever, encountered in disordered networks in *crystals*, affinity is the norm: the local symmetries, in fact, dictate that it should apply. The variable that is energy conjugate to the displacement gradient tensor (and therefore to Λ, too) is the first Piola-Kirchhoff stress tensor σ^I. The elastic energy required to deform an infinitesimal reference volume Ω of the system, which may be computed as

$$\mathcal{F} = \int_\Omega f(\Lambda) d^3\mathbf{x}, \tag{6}$$

may be used to compute the first Piola-Kirchhoff stress tensor by simple derivation of the energy density

$$\sigma^I_{ij} = \frac{\partial f(\Lambda)}{\partial \Lambda_{ij}}. \tag{7}$$

Because Λ is defined by derivatives of $\mathbf{R}$ with respect to positions in the reference volume, σ^I is a so-called mixed stress tensor—it measures the force in target space per unit area in reference space. Likewise, $f(\Lambda)$ is the elastic energy density defined relative to the reference volume Ω. Experiments, however, typically record the force in deformed space per unit area in the deformed space. The corresponding stress tensor is the true or Cauchy stress tensor σ^C. By using the facts that upon transforming to the reference space $\mathbf{x}$ the total elastic energy $\mathcal{F}$ should not change, that $d^3\mathbf{x} = (\det \Lambda)^{-1} d^3\mathbf{x}'$ and that $\partial_{\mathbf{x}'} = \Lambda^T \partial_{\mathbf{x}}$, we can compute the Cauchy stress from the first Piola-Kirchhoff stress directly as

$$\sigma^C = \frac{1}{\det \Lambda} \sigma^I \cdot \Lambda^T. \tag{8}$$

The strain measure conjugate to the Cauchy stress tensor is $\frac{\partial u_i}{\partial x'_\alpha}$, which is generally not simple to compute (it leads to the so-called Almansi strain tensor), and computing the Cauchy stress in general settings is typically most straightforwardly achieved by first computing $f(\Lambda)$, taking derivatives with respect to the components of Λ, and transforming the resultant σ^I to σ^C using Eq. (8). This is the procedure we will adopt in the following.

Note that this formalism applies equally to linearized elasticity theories and finite-strain systems. The constitutive behavior underlying the relation between stress and strain need not be linear (Hookean)—in fact, Eq. (7) derives from general thermodynamic considerations [26]. The assumption is made that the strain varies slowly over Ω but neither it, nor the stresses, need be small.

III. CAUCHY STRESS TENSOR FOR AN AFFINELY DEFORMING SPRING NETWORK

Consider now a network of springs subjected to a deformation Λ. The elastic energy density $f(\Lambda)$ for a volume Ω is then simply given by the sum of all contributions from individual springs:

$$f(\Lambda) = \frac{1}{\Omega} \sum_\alpha \varphi^\alpha(\Lambda). \tag{9}$$

The index α labels the springs, and $\varphi^\alpha(\Lambda)$ is the elastic energy of each single spring subject to Λ. For central force networks, this energy is a function of the *length* of the deformed spring only: denoting by $\mathbf{L}_\alpha$ the undeformed end-to-end vector of spring α we therefore have

$$\varphi^\alpha(\Lambda) = \varphi^\alpha(\|\Lambda \cdot \mathbf{L}^\alpha\|). \tag{10}$$

The first Piola-Kirchhoff stress tensor for such a network can be computed using Eq. (7):

$$\sigma^I_{ij} = \frac{\partial f(\Lambda)}{\partial \Lambda_{ij}} = \frac{1}{\Omega} \sum_\alpha \frac{\partial}{\partial \Lambda_{ij}} \varphi^\alpha(\|\Lambda \cdot \mathbf{L}^\alpha\|). \tag{11}$$

By the chain rule, the differential appearing in the summation may be rewritten:

$$\frac{\partial}{\partial \Lambda_{ij}}\varphi^{\alpha}(\|\Lambda\cdot\mathbf{L}^{\alpha}\|)=\left(\frac{\partial\varphi^{\alpha}(\|\Lambda\cdot\mathbf{L}^{\alpha}\|)}{\partial\|\Lambda\cdot\mathbf{L}^{\alpha}\|}\right)\left(\frac{\partial\|\Lambda\cdot\mathbf{L}^{\alpha}\|}{\partial\Lambda_{ij}}\right).$$

The first term between brackets is simply the derivative of the spring energy with respect to the spring length— i.e., the *force* as a function of the length $\tau^{\alpha}(\|\Lambda\cdot\mathbf{L}^{\alpha}\|)$. The second term may be rewritten as

$$\begin{aligned}&\frac{\partial\|\Lambda\cdot\mathbf{L}^{\alpha}\|}{\partial\Lambda_{ij}}\\&=\frac{\partial}{\partial\Lambda_{ij}}\left(\Lambda_{kl}\mathbf{L}^{\alpha}_{l}\Lambda_{km}\mathbf{L}^{\alpha}_{m}\right)^{1/2}\\&=\frac{1}{2\|\Lambda\cdot\mathbf{L}^{\alpha}\|}\left(\delta_{ki}\delta_{lj}\mathbf{L}^{\alpha}_{l}\Lambda_{km}\mathbf{L}^{\alpha}_{m}+\Lambda_{kl}\mathbf{L}^{\alpha}_{l}\delta_{ki}\delta_{mj}\mathbf{L}^{\alpha}_{m}\right)\\&=\frac{(\Lambda\cdot\mathbf{L}^{\alpha})_i(\mathbf{L}^{\alpha})_j}{\|\Lambda\cdot\mathbf{L}^{\alpha}\|},\end{aligned}\tag{12}$$

so that the components of the first Piola-Kirchhoff stress tensor for the network are given by

$$\sigma^{I}_{ij}=\frac{1}{\Omega}\sum_{\alpha}\tau^{\alpha}(\|\Lambda\cdot\mathbf{L}^{\alpha}\|)\left(\frac{(\Lambda\cdot\mathbf{L}^{\alpha})_i(\mathbf{L}^{\alpha})_j}{\|\Lambda\cdot\mathbf{L}^{\alpha}\|}\right).\tag{13}$$

Recalling that we may transform σ^{I} to the Cauchy stress σ^{C} using Eq. (8), we find

$$\sigma^{C}_{ij}=\frac{1}{\Omega\,\det\Lambda}\sum_{\alpha}\tau^{\alpha}(\|\Lambda\cdot\mathbf{L}^{\alpha}\|)\left(\frac{(\Lambda\cdot\mathbf{L}^{\alpha})_i(\Lambda\cdot\mathbf{L}^{\alpha})_j}{\|\Lambda\cdot\mathbf{L}^{\alpha}\|}\right).\tag{14}$$

We now pass to a continuum limit, replacing the sum by an integral over the distribution $\mathcal{P}(\mathbf{L})$ of undeformed end-to-end lengths:

$$\sum_{\alpha=1}^{N}g(\mathbf{L}^{\alpha})\longrightarrow N\langle g(\mathbf{L})\rangle=N\int\mathcal{P}(\mathbf{L})g(\mathbf{L})d^{3}\mathbf{L}.\tag{15}$$

Letting ρ denote the number density of springs in the reference configuration, i.e., $\rho=N/\Omega$, this yields the expression for the Cauchy stress appropriate for large spring networks:

$$\sigma^{C}_{ij}=\frac{\rho}{\det\Lambda}\int\mathcal{P}(\mathbf{L})\tau(\|\Lambda\cdot\mathbf{L}\|)\left(\frac{(\Lambda\cdot\mathbf{L})_i(\Lambda\cdot\mathbf{L})_j}{\|\Lambda\cdot\mathbf{L}\|}\right)d^{3}\mathbf{L}.\tag{16}$$

The integral is over all of 3-space. A nonlinear dependence of the stress tensor component σ^{C}_{ij} on the strain Λ may thus originate from two sources: a nonlinear force-extension curve *or* a geometrically incurred nonlinearity arising from the second bracketed term in the integral—this term does not depend on the force-extension behavior. The prefactor is ρ_{Λ}, the number density in the deformed configuration:

$$\rho_{\Lambda}=\left(\frac{N}{\Omega}\right)\left(\frac{\Omega}{\Omega'}\right)=\frac{\rho}{\det\Lambda}.\tag{17}$$

Equation (16) does not assume isotropy; in fact, $\mathcal{P}(\mathbf{L})$ may take on any form including the collection of δ peaks appropriate for crystalline structures. Provided one knows the force-extension curve, the initial radial distribution of spring end-to-end vectors, and, obviously, the strain Λ this expression allows one to directly compute, to all desired nonlinear orders, the affine Cauchy stress.

IV. SHEAR AND NORMAL STRESSES FOR AN AFFINE NETWORK WITH TUNABLY ASYMMETRIC SPRINGS

To investigate the general role of the asymmetry of the force-extension curve, we consider an isotropic, affinely deforming network composed of identical nonlinear springs whose force-extension behavior contains a term quadratic in the extension. We shall term this model the *quad spring*. Its force extension is given by

$$\tau(\mathbf{L})=k_1(\|\mathbf{L}\|-\ell_0)+\tfrac{1}{2}k_2(\|\mathbf{L}\|-\ell_0)^2.\tag{18}$$

The rest length ℓ_0 and the two mechanical constants k_1 and k_2 fully characterize the spring's elastic response; k_1 is the familiar linear (Hookean) spring constant. The quadratic term is introduced to allow for the possibility of breaking the $\delta L\rightarrow-\delta L$ antisymmetry (δL being $\|\mathbf{L}\|-\ell_0$, the deviation from equilibrium). Mechanical stability requires that

$$\frac{\partial\tau(L)}{\partial L}\geqslant 0\Rightarrow k_1+k_2\delta L\geqslant 0\quad\forall\delta L.\tag{19}$$

Which implies that $k_1>0$ is always required for mechanical stability, and that negative values for k_2 introduce a maximal extensional strain $\varepsilon_{\max}=(\ell-\ell_0)/\ell_0=|k_1/(k_2\ell_0)|$ beyond which an elastic instability occurs. In what follows, we will consider isotropic, perfectly monodisperse filament networks—the radial distribution for which is (in three dimensions)

$$\mathcal{P}(\mathbf{L})=\frac{1}{4\pi\ell_0^2}\delta(\|\mathbf{L}\|-\ell_0).\tag{20}$$

With this choice for the radial distribution, each of the filaments is at its rest length and the material is thus prepared in a stress-free reference state. In the following, and in particular in the numerical simulations, we shall work with such unstressed reference states unless explicitly stated otherwise. The affine formalism described here, however, does not assume or require the absence of prestresses and towards the end of this section we briefly discuss the effects of pressurizing the system. Throughout this paper, we will consider the response of materials to *simple shear* deformations. These are of particular relevance, as a standard rheology experiment in cone-plate geometry imparts this deformation to infinitesimal volumes of the sample. For a simple shear of dimensionless magnitude γ (the shear strain) in the $\hat{x}\hat{z}$ direction, the Cauchy deformation tensor $\Lambda(\gamma)$ is given by

$$\Lambda(\gamma)=\begin{pmatrix}1&0&\gamma\\0&1&0\\0&0&1\end{pmatrix}.\tag{21}$$

Thus, with $\tau(\mathbf{L})$, $\mathcal{P}(\mathbf{x})$, and Λ specified, we may compute the full nonlinear Cauchy stress tensor. This is most straightforwardly done in spherical coordinates, and amounts to little more than evaluating Eq. (16). This must be done numerically for arbitrary shear strain γ, but the high- and low-strain limits may be obtained analytically. Let us consider small strains.

Expanding Eq. (16) to first order in γ yields the following for $\hat{x}\hat{z}$ stress:

$$\sigma_{xz}^{C} \approx \left(\frac{\rho k_1 \ell_0^2}{4\pi}\right)\gamma \int_0^{\pi} d\theta \int_0^{2\pi} d\varphi[\cos^2\theta \, \sin^3\theta \, \cos^2\varphi] = \left(\frac{1}{15}\rho k_1 \ell_0^2\right)\gamma \equiv \sigma_{xz,\mathrm{lin}}^{C}. \quad (22)$$

We recognize here the familiar expression for the shear modulus of a Hookean spring network, as defined by the small-strain relation $\sigma_{xz}^{C} = \mathsf{G}\gamma$:

$$\mathsf{G}_{\mathrm{spring}}^{3D} = \tfrac{1}{15}\rho k_1 \ell_0^2. \quad (23)$$

The appearance of this Hookean modulus makes sense—the nonlinear effects introduced by a nonzero k_2 can enter only at $O(\gamma^2)$. We may also compute the first correction term to this linear response by expanding the entire integrand to third order in γ (the quadratic term is zero because the $\hat{x}\hat{z}$ shear stress is antisymmetric in the strain). This yields a correction

$$\sigma_{xz}^{C} - \sigma_{xz,\mathrm{lin}}^{C} = \left(\tfrac{2}{105}\rho(2k_1 + k_2\ell_0)\ell_0^2\right)\gamma^3. \quad (24)$$

If the stress rises faster than linear, i.e., if $2k_1 + k_2\ell_0 > 0$, the network is said to be strain stiffening; with a differential modulus that rises with increasing strain. If this condition is not satisfied, it is strain softening. Since $k_1 > 0$, the generic tendency is towards stiffening and a network of Hookean springs will stiffen geometrically. For the normal stresses, which must be symmetric in γ and therefore can appear only at $O(\gamma^2)$, we must expand Eq. (16) to second order. This yields

$$\sigma_{xx}^{C} \approx \left(\tfrac{1}{210}\rho(26k_1 + 3k_2\ell_0)\ell_0^2\right)\gamma^2, \quad (25)$$

$$\sigma_{yy}^{C} \approx \left(\tfrac{1}{210}\rho(4k_1 + k_2\ell_0)\ell_0^2\right)\gamma^2, \quad (26)$$

$$\sigma_{zz}^{C} \approx \left(\tfrac{1}{70}\rho(4k_1 + k_2\ell_0)\ell_0^2\right)\gamma^2. \quad (27)$$

In general, the first normal stress *difference* $\sigma_{xx}^{C} - \sigma_{zz}^{C}$ is recorded in a rheometer. The curved deformation geometry in the $\hat{x}\hat{x}$ direction sets up hoop stresses, which are balanced by a radial pressure gradient in an incompressible material (giving rise to the curious rod climbing effect) and thus contribute to the vertical thrust. However, for the open, semiflexible networks that we seek to describe here, we assume that these hoop stresses—unconstrained by the moving plates of the rheometer—relax more quickly than the $\hat{z}\hat{z}$ stresses. This, we speculate, might arise due to a difference in length scales between the radial and gap directions in cone-and-plate setups, or to nonaffine motion of the network relative to the solvent which is most pronounced at low frequencies [27]. In the Appendix, we show by explicit calculation that allowing the $\hat{x}\hat{x}$ stress to relax leads to the same conclusions as those presented here. Thus, in the limit of slow, quasistatic driving, we assume the recorded thrust is dominated by the $\hat{z}\hat{z}$ component of the stress. In this respect, we follow the conventions in [22–24,28], which were shown to agree very well with cone-plate rheometry measurements on a multitude of open semiflexible hydrogels (actin, collagen, fibrin, neurofilaments, and matrigel). We do note that, although the models assuming $\hat{z}\hat{z}$ dominance capture the normal stress measurements quite well, we are not aware of any separate validation—experimental or theoretical—of the differential relaxation of hoop and normal stresses. For high-frequency driving, fast compared even to the relaxation time of the hoop stresses, we expect to see the thrust crossover from $-\sigma_{zz}^{C}$ to $\sigma_{xx}^{C} - \sigma_{zz}^{C}$, the latter of which, generically, is *positive* rather than negative. We are not aware of any published experiments that could confirm this prediction for semiflexible networks, but it would be very interesting to do so—the driving frequency might provide yet another handle to manipulate and modify the normal response of network materials. In what follows, however, we shall work in the low-frequency limit. A note concerning the sign of the normal stress: the Cauchy stress tensor as used here quantifies the force per unit area in the material's deformed configuration required to hold it in the deformed shape. A positive $\hat{z}\hat{z}$-stress tensor component thus implies a force in the positive $\hat{z}$ direction is required to maintain the sheared shape, i.e., the material itself is pulling the top surface inward. Materials exhibiting this kind of behavior are said to display *negative normal stress*. Evidently, provided that

$$4k_1 + k_2\ell_0 > 0, \quad (28)$$

the quad spring network exhibits negative normal stress—see Fig. 1. Interestingly, even in the absence of a nonlinear term—i.e., for a network composed of perfectly linear Hookean springs—the network displays negative normal stresses: mechanical stability of the individual springs requires a positive k_1. Again, this nonlinear effect cannot be due to the force-

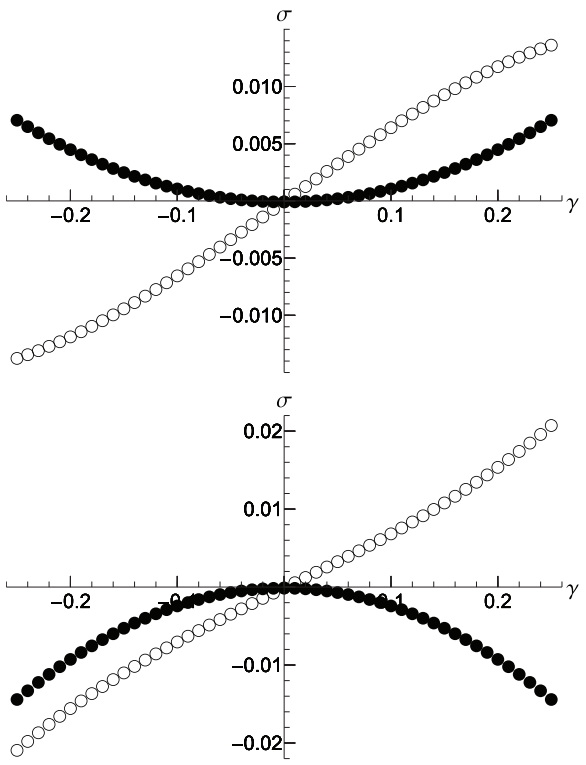

FIG. 1. Normal (•) and shear stresses (○) versus shear strain γ for the quad spring network. The normal stresses σ_{zz}^{C} in the quad spring model can be either positive or negative, depending on the relative magnitude of k_1 and k_2. Upper image: $k_1 = 1, k_2 = -12$ (positive normal stress). Lower image: $k_1 = 1, k_2 = 12$ (negative normal stress). Note the expected symmetries: the normal stress σ_{zz}^{C} is an even function of the shear strain γ; the shear stress σ_{xz}^{C} is odd.

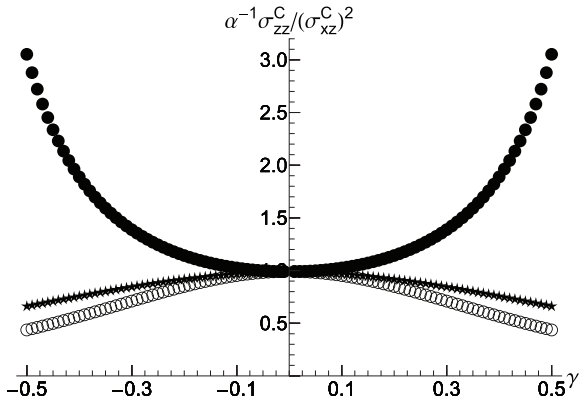

FIG. 2. Scaling plot of the ratio of normal to squared shear stresses $\alpha^{-1}\sigma^C_{zz}/(\sigma^C_{xz})^2$ for $k_1 = 1$, $\ell_0 = 1$, and $k_2 = -8(\bullet), 5(\star), 1(\circ)$.

extension relation and is therefore purely geometric in origin. One may wish to note, also, that even the linear, Hookean force-extension relation produces higher-order terms when its network energy is expanded in the node displacements as soon as the rest lengths are nonzero. In particular, we conclude that negative normal stresses do not require an asymmetric force-extension relation. A convenient way to check the small strain asymptotics is by inspecting the relation between the $\hat{x}\hat{z}$ and $\hat{z}\hat{z}$ stresses:

$$\sigma^C_{zz} = \alpha\left(\sigma^C_{xz}\right)^2, \quad \text{with} \quad \alpha = \frac{45}{14}\frac{1}{\rho\ell_0^2}\left(\frac{4k_1 + k_2\ell_0}{k_1^2}\right). \tag{29}$$

Indeed, Fig. 2 shows that the ratio $\alpha^{-1}\sigma^C_{zz}/(\sigma^C_{xz})^2$ approaches unity for small strains. In practice, this may be used to determine the α factor from experiments and compare it to single-molecule force-extension data, particularly as k_1 may be extracted from the small-strain behavior of σ^C_{xz}.

Equation (16) may also be used to assess the effects of uniform prestress on affinely deforming spring networks. To do so, we apply a uniform dilation (or compression) to an initially stress-free network by replacing $\ell_0 \to (1+\lambda)\ell_0$ in Eq. (20). The same computations as before yield that doing so produces identical, nonzero diagonal stress tensor components at zero shear stress:

$$\begin{aligned}\sigma^C_{xx}(\gamma = 0, \lambda \neq 0) &= \sigma^C_{yy}(\gamma = 0, \lambda \neq 0) \\ &= \sigma^C_{zz}(\gamma = 0, \lambda \neq 0) \\ &\approx \tfrac{1}{3}k_1\ell_0^2\rho\lambda \equiv \Pi_0(\lambda)\end{aligned} \tag{30}$$

and is thus equivalent to introducing a uniform pressure $\Pi_0(\lambda)$ in the system, whose magnitude is proportional to the dilation λ. At finite shear strain, we may also compute the corrections to the normal stress which yields, to first order in λ,

$$\sigma^C_{zz}(\gamma,\lambda) - \sigma^C_{zz}(\gamma,0) \approx \Pi_0(\lambda) + \frac{\ell_0^2\rho}{210}(21k_2\ell_0 + 12k_1)\gamma^2\lambda. \tag{31}$$

Thus pressurizing the affine system augments the normal stress response in a strain-dependent manner, at lowest nontrivial order in γ. Depending on the signs and relative magnitudes of k_1, k_2 and the applied strain γ, this correction may be positive or negative, which opens up interesting possibilities to manipulate the normal stress response by externally applied strains.

Summarizing the behavior of the (initially stress-free) quad spring network, we find that both negative (NNS) and positive (PNS) normal stresses are possible, as well as both strain stiffening and strain softening—depending on the values of k_1, k_2, and ℓ_0:

$$\begin{aligned} k_2 < -\frac{4k_1}{\ell_0}: &\quad \text{softening, PNS,} \\ -\frac{4k_1}{\ell_0} < k_2 < -\frac{2k_1}{\ell_0}: &\quad \text{softening, NNS,} \\ k_2 > -\frac{2k_1}{\ell_0}: &\quad \text{stiffening, NNS.}\end{aligned}$$

V. NORMAL STRESSES FOR AN AFFINE SEMIFLEXIBLE WORMLIKE CHAIN NETWORK

To what extent is the negative normal stress exhibited by biopolymer networks determined by geometry and/or nonlinear force-extension behavior? In order to address this, first under the assumption of affine deformations, we consider the analytical expression for the extension-force relation as reported in, for instance, Ref. [6],

$$\mathbf{L}(\tau) = \ell_c - \frac{k_B T}{2\tau}\left[\sqrt{\frac{\tau\ell_c^2}{k_B T \ell_p}}\coth\left(\sqrt{\frac{\tau\ell_c^2}{k_B T\ell_p}}\right) - 1\right],$$

where ℓ_p is the persistence length and ℓ_c is the contour length. The equilibrium length of this polymer is computed as

$$\ell_0 = \mathbf{L}(0) = \ell_c\left(1 - \frac{\ell_c}{6\ell_p}\right). \tag{32}$$

While an analytical inversion to obtain the force-extension relationship $\tau(\mathbf{L})$ is impossible, we may systematically obtain all orders of its expansion around $\mathbf{L} = \ell_0$, from which we can infer the appropriate expressions for k_1 and k_2 to compare to our quad spring network. Doing so yields

$$k_1 = 90k_B T\frac{\ell_p^2}{\ell_c^4}, \quad k_2 = \frac{2700}{7}k_B T\frac{\ell_p^3}{\ell_c^6} = \frac{30}{7}\frac{\ell_p}{\ell_c^2}k_1. \tag{33}$$

Since both k_1 and k_2 are positive for an affine semiflexible network, it is expected to exhibit both strain stiffening and negative normal stresses. The relative contributions of geometry and nonlinear force extension, from Eq. (27), are given by the ratio

$$\frac{4k_1}{k_2\ell_0} = \frac{28\ell_c}{5(6\ell_p - \ell_c)}. \tag{34}$$

For polymers that have $\ell_p \sim \ell_c$, this ratio is nearly one—for such networks, the geometric and elastic nonlinearities are of equal inportance in determining the magnitude of the normal stress. For actin networks, however, one generally finds that $\ell_c \ll \ell_p$, and the ratio drops rapidly suggesting that in actin gels the normal stresses are dictated chiefly by the elastic nonlinearity of the fibers. For the fibrin networks considered in [22], the persistence length is considerably smaller but the typical contour length is difficult to estimate.

While the quad spring network is indefinitely extensible, the semiflexible wormlike chain exhibits a divergence in both the

shear and normal stresses as the critical strain γ_c is approached. This is the shear strain for which the first filament reaches full extension. For an affinely deforming semiflexible system, this critical strain can be computed analytically and equals

$$\gamma_c = \frac{\ell_c}{6\ell_p}\left(\frac{12\ell_p - \ell_c}{6\ell_p - \ell_c}\right). \tag{35}$$

For the small strain regime, symmetry still dictates that $\sigma^C_{zz} \sim \gamma^2 \sim (\sigma^C_{xz})^2$, but close to the strain threshold the force will diverge characteristically as

$$\tau \sim \frac{1}{(\gamma_c - \gamma)^2}. \tag{36}$$

The geometric factor in Eq. (16), in the large strain limit, vanishes as γ^{-1} for the $\hat{z}\hat{z}$ component, and approaches unity for the $\hat{x}\hat{z}$ component. As a result, the ratio of normal to shear stress has an asymptotic regime in which

$$\frac{\sigma^C_{zz}}{\sigma^C_{xz}} \sim \lim_{\gamma\to\gamma_c}\left(\frac{1}{\gamma(\gamma_c-\gamma)^2}\right)\left(\frac{1}{(\gamma_c-\gamma)^2}\right)^{-1} = \frac{1}{\gamma_c}. \tag{37}$$

In other words, for large strains the normal stress becomes linearly proportional to the shear stress, and indeed such a crossover from a quadratic ratio to a linear ratio is observed for a wide class of biopolymer gels in the experiments reported in [22]. For stiffer networks, γ_c decreases rapidly and the normal stresses may indeed become significantly larger than the shear stresses. It would be interesting to determine experimentally whether indeed the stiffer biopolymer networks exhibit the largest ratios of normal to shear stress, and whether this increase correlates with the critical shear strain.

VI. NORMAL AND SHEAR STRESSES IN NONAFFINELY DEFORMING NETWORKS

To assess to what extent our findings for affinely deforming networks hold up when nonaffinity and bending contributions are present we turn to numerical simulations. We consider the so-called Mikado network [25]: a random, two-dimensional (2D) arrangement of polymers whose energy involves both bending and stretching:

$$\mathcal{E} = \sum_{\text{all chains}}\left(\kappa\sum_{\langle ijk\rangle}\frac{\Theta^2_{ijk}}{\ell_{ij}+\ell_{jk}} + \frac{\mathsf{Y}}{2}\sum_{\langle ij\rangle}\frac{(\ell_{ij}-\ell^0_{ij})^2}{\ell^0_{ij}}\right).$$

In this expression, ℓ_{ij} is the length of segment ij linking nodes i and j, and ℓ^0_{ij} is the rest length of this segment. Θ_{ijk} is the angle between segments ij and jk, and the summations within each polymer run over triplets of connected nodes along the same polymer $\langle ijk\rangle$ for the angles and doublets of nodes connected along the same polymer $\langle ij\rangle$ for the extensions. κ is the bending rigidity, and Y is the modulus—the spring constant for each segment is computed as $k_{ij} = \mathsf{Y}/\ell^0_{ij}$. This representation amounts to the discrete persistent chain model [28], and may be thought of as a discrete version of an extensible wormlike chain (WLC). By mapping its linear elastic response onto that of the WLC the coefficients κ and Y may be matched to the persistence length and the extensional modulus of a continuum WLC [28–30].

We generate many different configurations of the Mikado network [25], and subject its boundaries to the same simple shear deformation $\Lambda(\gamma)$. The positions of the cross-linkers are then determined using a nonlinear conjugate gradient algorithm [31]. This yields the nonaffine energy as a function of the shear strain $\mathcal{E}_{\text{NA}}(\gamma)$. This energy is graphed in Fig. 3, which shows the general effect of nonaffinity: as we increase the ratio κ/Y, the strain energy at a given value of the shear strain increases towards, but never reaches, its affine value $\mathcal{E}_{\text{A}}(\gamma)$. This is a crucially important feature: even in the limit of infinitely stiff segments, the system does not become affine. While the distinction between affine and nonaffine is often summarized as bending (nonaffine) vs stretching (affine) dominated systems, there are additional nonaffine modes of deformation which do not involve bending: rotation of filaments and translation. These modes are not suppressed by increasing the bending rigidity, and therefore even the infinitely stiff system possesses more degrees of freedom than its affinely constrained counterpart.

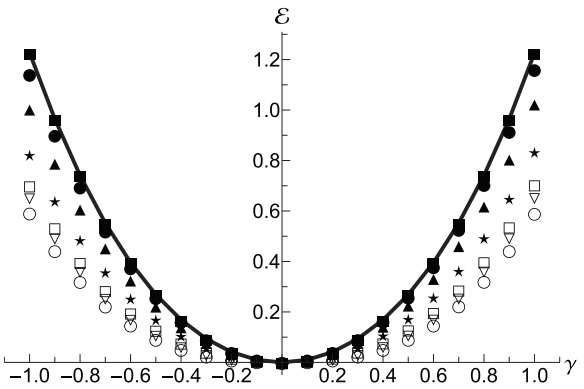

FIG. 3. Affine and nonaffine energies $\mathcal{E}$ versus shear strain γ for networks with different stiffnesses. The upper curve (■) corresponds to the affine case, while lower curves correspond to various bending stiffnesses $\kappa/\mathsf{Y} = 10^{-1}$(●), $\kappa/\mathsf{Y} = 10^{-2}$(▲), $\kappa/\mathsf{Y} = 10^{-3}$(⋆), $\kappa/\mathsf{Y} = 10^{-4}$(□), $\kappa/\mathsf{Y} = 10^{-5}$(▽), and $\kappa/\mathsf{Y} = 10^{-6}$(○). Filament rigidity decreases from top to bottom. Note that nonaffinity induces a softer response spanning the entire spectrum of the bending rigidity.

From each of these energy curves, we may directly compute the $\hat{x}\hat{z}$ component of the Cauchy stress as

$$\sigma^C_{xz} = \frac{\partial\mathcal{E}_{\text{NA}}(\gamma)}{\partial\gamma}. \tag{38}$$

The normal stresses are obtained by superimposing, on the simple 2D shear deformation $\Lambda(\gamma)$, an infinitesimal uniaxial extension in the $\hat{z}$ direction:

$$\Lambda'(\gamma,\alpha) = \begin{pmatrix} 1 & \gamma \\ 0 & 1+\alpha \end{pmatrix}, \tag{39}$$

which yields a nonaffine strain energy function of two variables $\mathcal{E}'_{\text{NA}}(\gamma,\alpha)$, from which we compute the $\hat{z}\hat{z}$ component of the Cauchy stress as

$$\sigma^C_{zz} = \frac{\partial\mathcal{E}'_{\text{NA}}(\gamma,0)}{\partial\alpha}. \tag{40}$$

The results for the shear and normal stresses in the nonaffine Mikado model are collected in Fig. 4 and Fig. 5. We recover the surprising behavior also reported by [23]: while the shear stress σ^C_{xz} rises towards its affine value for increasing bend

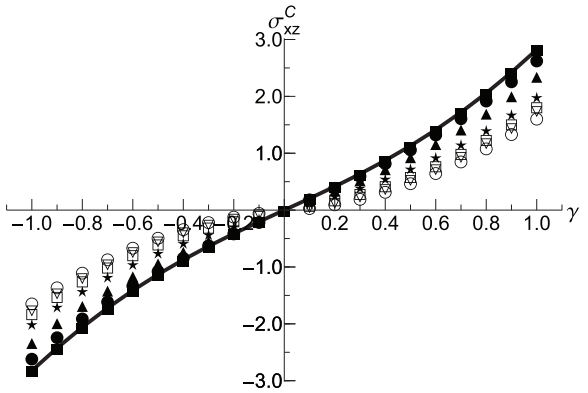

FIG. 4. Affine and nonaffine shear stresses σ^C_{xz} versus applied shear strain γ for networks with different stiffnesses. The upper (lower) curve for positive (negative) applied shear strain (■) corresponds to the affine case, while lower (upper) curves correspond to various bending stiffnesses $\kappa/\mathsf{Y} = 10^{-1}$(●), $\kappa/\mathsf{Y} = 10^{-2}$(▲), $\kappa/\mathsf{Y} = 10^{-3}$(⋆), $\kappa/\mathsf{Y} = 10^{-4}$(□), $\kappa/\mathsf{Y} = 10^{-5}$(▽), and $\kappa/\mathsf{Y} = 10^{-6}$(○). Shear stresses increase with increasing bending stiffness.

stiffness κ, the normal stress does exactly the opposite and decreases. These two tendencies may appear, at first sight, to be contradictory: if the shear stress approaches the affine result, one might conclude that the network must be deforming ever more affinely and that, consequently, the normal stress should also approach its affine limit. This reasoning is flawed for the same reason as mentioned above: while the energy of the nonaffinely deforming system increases for increasing bending rigidity, it does not asymptote to the affine curve for infinite κ/Y. The remaining nonaffinity due to rotations and translations of fibers conspire to lower the normal stresses while raising the shear stresses. Symmetry still dictates that $\sigma^C_{zz} \sim \gamma^2 \sim (\sigma^C_{xz})^2$ for small γ, as depicted in Fig. 6. Although these networks do not possess a limited extensibility, they still exhibit a transition from quadratic to a linear normal-to-shear stress ratio for large strains, but do so dissimilarly to the affine wormlike chain model. For these networks, softer systems reach a linear normal-to-shear stress ratio at strains lower than their more rigid counterparts.

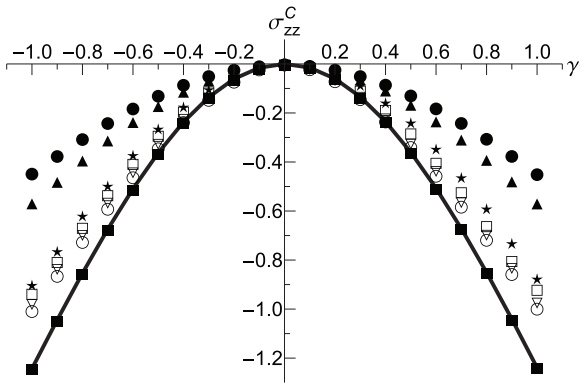

FIG. 5. Affine and nonaffine normal stresses σ^C_{zz} versus applied shear strain γ for networks with different stiffnesses. The lower curve (■) corresponds to the affine case, while upper curves correspond to various bending stiffnesses $\kappa/\mathsf{Y} = 10^{-1}$(●), $\kappa/\mathsf{Y} = 10^{-2}$(▲), $\kappa/\mathsf{Y} = 10^{-3}$(⋆), $\kappa/\mathsf{Y} = 10^{-4}$(□), $\kappa/\mathsf{Y} = 10^{-5}$(▽), and $\kappa/\mathsf{Y} = 10^{-6}$(○). Note that normal stresses decrease with increasing bending stiffness.

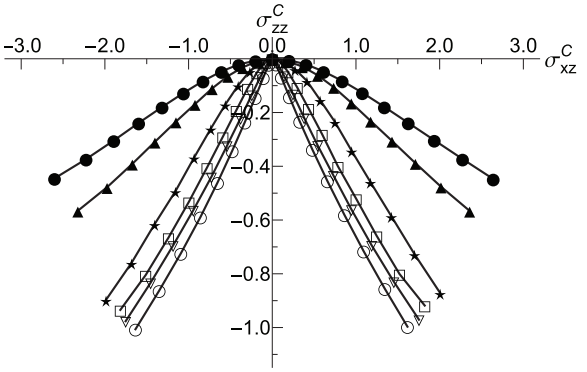

FIG. 6. Normal stresses σ^C_{zz} plotted versus their corresponding shear stresses σ^C_{xz} for various bending stiffnesses $\kappa/\mathsf{Y} = 10^{-1}$(●), $\kappa/\mathsf{Y} = 10^{-2}$(▲), $\kappa/\mathsf{Y} = 10^{-3}$(⋆), $\kappa/\mathsf{Y} = 10^{-4}$(□), $\kappa/\mathsf{Y} = 10^{-5}$(▽), and $\kappa/\mathsf{Y} = 10^{-6}$(○). All networks show a crossover from a quadratic to linear normal-to-shear stress ratio when transitioning from small to large deformations.

VII. NONAFFINITY: GENERAL CONSIDERATIONS

Note that while $\mathcal{E}_{\rm NA}(\gamma) \leqslant \mathcal{E}_{\rm A}(\gamma)$ for all values of the shear strain γ, a similar relation need not hold for the stresses: it is possible and allowed for the nonaffine shear or normal stress to be larger or smaller than its affine counterpart. We may, however, expand both the affine and nonaffine energies to second order around their equilibrium, $\gamma = 0$ values (which are zero, in each case) to conclude that

$$\frac{\partial^2 \mathcal{E}_{\rm A}}{\partial \gamma^2} \geqslant \frac{\partial^2 \mathcal{E}_{\rm NA}}{\partial \gamma^2}, \tag{41}$$

and therefore that the linear shear modulus $G^0_{\rm A}$ for the affine material must be larger than that of the nonaffine material $G^0_{\rm NA}$. Equality holds only when all nonaffine degrees of freedom are effectively constrained (this happens, for instance, in the limit where the filament lengths become of the order of the system size). Our simulations, however, are well below this limit. Figure 7 brings out the overall trend: even for very rigid (averaged) configurations, shear moduli are lower than their

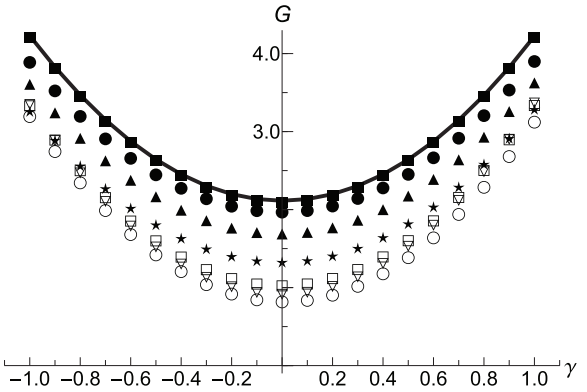

FIG. 7. Affine and nonaffine shear moduli G versus shear strain γ for networks with different stiffnesses. The upper curve (■) corresponds to the affine case, while lower curves correspond to various bending stiffnesses $\kappa/\mathsf{Y} = 10^{-1}$(●), $\kappa/\mathsf{Y} = 10^{-2}$(▲), $\kappa/\mathsf{Y} = 10^{-3}$(⋆), $\kappa/\mathsf{Y} = 10^{-4}$(□), $\kappa/\mathsf{Y} = 10^{-5}$(▽), and $\kappa/\mathsf{Y} = 10^{-6}$(○). Affine shear moduli are larger than all their nonaffine counterparts.

affine correspondent, and, in general, even for small strain the bending, rotational, and translational degrees of freedom effect a finite drop in modulus, as many previous simulation studies including our own have confirmed [28]. This reinforces an essential point: even at infinitesimal strains, the nonaffinity is not negligible. In the presence of nonaffinity—an all but unavoidable companion of disorder in network materials—the linear mechanical response is dictated by the small strain, but *finite* nonaffinity, limit of the elastic energy.

VIII. CONCLUSION

The normal stresses that arise in cross-linked elastic networks are determined and modulated by three distinct, but not independent, mechanisms. The first is geometric nonlinearity: the differential stretching and reorienting of network constituents depending on their orientation in space. The second is elastic nonlinearity: The concave (or convex) nonlinear force-extension relation of polymers as reflected in models like the FJC and the WLC. The third factor is nonaffinity: the tendency for bulk cross-linkers to move relative to the deformation of the boundary.

In a simple nonlinear elastic model that permits the analytical calculation of (Cauchy) stresses, we observe that at low frequencies the sign of the normal stress and the nonlinear shear stress response are not decoupled: depending on the relative magnitude (and signs) of the second and fourth shear strain derivatives of the strain energy the stiffening of softening behavior is linked to positive or negative normal stresses.

Our work suggests that by manipulating the three mechanisms giving rise to negative normal stresses the normal response of network materials may be modulated. In particular, the driving frequency, prestresses in the form of external pressures, and the ratio between the stretch and bend stiffness may each be modified in biopolymeric or synthetic gels to control their nonlinear mechanical properties.

In numerical simulations of Mikado networks we find that nonaffine displacements preserve the overall tendencies observed in the affine system, but that both shear and stress tensor components are modified by the presence of nonaffinity. Interestingly, it affects shear and normal stresses in opposite fashion: shear stresses rise as nonaffinely deforming systems become increasingly rigid, while normal stresses decrease. This highlights the importance of nonbending contributions to nonaffinity, which are responsible for finite shifts even in the linear elastic response regime. In the presence of nonaffinity, even the linear theory of network elasticity must therefore be augmented to allow for a finite amount of nonaffine displacement, which brings into question the relevance of the affinely deforming system as a meaningful reference configuration, or as a valid point of departure for perturbative approaches.

ACKNOWLEDGMENTS

We thank F. C. MacKintosh, H. E. Amuasi, M. A. J. Michels, R. W. Ogden, J. Douglas, E. M. Spiesz, and an anonymous referee for valuable discussions and suggestions. This work was generously supported by the Institute for Complex Molecular Systems (ICMS) at Eindhoven University of Technology.

APPENDIX: EFFECT OF RELAXING σ^C_{xx} ON σ^C_{zz}

Assuming that the $\hat{z}\hat{z}$ component of the stress tensor dominates the first normal stress difference—as is routinely done in modeling normal stresses—presumes that the $\hat{x}\hat{x}$ component of the stress tensor is able to relax. This relaxation, in turn, affects the $\hat{z}\hat{z}$ stress. In this appendix, we compute this effect within the context of the affine quad spring model. To do so, we consider a wider class of deformations, parametrized by a deformation matrix:

$$\tilde{\Lambda}(\varepsilon,\gamma) = \begin{pmatrix} 1+\varepsilon & 0 & \gamma \\ 0 & 1 & 0 \\ 0 & 0 & 1 \end{pmatrix}. \tag{A1}$$

The additional parameter ε is used to adjust the length in the $\hat{x}$ direction of the system, and will be used in the following to allow σ^C_{xx} to relax to zero. Under the action of $\tilde{\Lambda}$, we may compute the $\hat{x}\hat{x}$ component of the stress tensor using Eq. (16) to be, to second order in γ and first order in ε,

$$\sigma^C_{xx}(\varepsilon,\gamma) \approx \left(\tfrac{1}{210}\rho(26k_1+3k_2\ell_0)\ell_0^2\right)\gamma^2 \tag{A2}$$

$$+\varepsilon\left(\tfrac{1}{210}\rho(42k_1+28k_1\gamma^2+17k_2\ell_0\gamma^2)\ell_0^2\right). \tag{A3}$$

Solving for $\sigma^C_{xx}(\varepsilon^\star,\gamma)=0$, we find that full relaxation of the $\hat{x}\hat{x}$ stress is achieved by choosing

$$\varepsilon^\star = \frac{-26k_1\gamma^2 - 3k_2\ell_0\gamma^2}{42k_1+28k_1\gamma^2+17k_2\ell_0\gamma^2}. \tag{A4}$$

Thus, by deforming the material according to $\tilde{\Lambda}(\varepsilon^\star,\gamma)$, we may compute the Cauchy stresses as they develop in the strict absence of hoop stresses. Note that ε is generally negative (particularly for $k_2=0$): while relaxing, the material contracts along the $\hat{x}$ direction as was to be expected. We again use Eq. (16) to find that

$$\sigma^C_{zz}(\varepsilon^\star,\gamma) \approx \left(\tfrac{1}{315}\rho(5k_1+3k_2\ell_0)\ell_0^2\right)\gamma^2. \tag{A5}$$

Evidently, when the hoop stress is relaxed the normal stress, which is now exactly equal to the first normal stress difference and $-\sigma^C_{zz}$, may still be positive or negative, depending on the sign of the combination $(5k_1+3k_2\ell_0)$. Likewise, for a strictly linear spring network the geometrical nonlinearity still leads to generic negative normal stress. Thus, our findings, though numerically slightly different, remain valid when the stress is relaxed. A caveat is still in order—what we show here is that *when* the $\hat{x}\hat{x}$ stresses relax the normal stress behavior remains as we predict. We cannot say whether, in practice, they *can* or *will* relax. For completeness, we note that the remaining stress tensor components, computed in completely analogous fashion, read

$$\sigma^C_{xx}(\varepsilon^\star,\gamma) = 0, \tag{A6}$$

$$\sigma^C_{yy}(\varepsilon^\star,\gamma) \approx -\left(\tfrac{1}{45}\rho k_1\ell_0^2\right)\gamma^2, \tag{A7}$$

$$\sigma^C_{xz}(\varepsilon^\star,\gamma) \approx \left(\tfrac{1}{15}\rho k_1\ell_0^2\right)\gamma. \tag{A8}$$

[1] E. M. Huisman, T. van Dillen, P. R. Onck, and E. Van der Giessen, Phys. Rev. Lett. **99**, 208103 (2007).
[2] M. Plischke and B. Joós, Phys. Rev. Lett. **80**, 4907 (1998).
[3] C. Heussinger, B. Schaefer, and E. Frey, Phys. Rev. E **76**, 031906 (2007).
[4] I. E. Zarraga, D. A. Hill, and D. T. Leighton, J. Rheol. **44**, 185 (2000).
[5] M. L. Gardel, M. T. Valentine, J. C. Crocker, A. R. Bausch, and D. A. Weitz, Phys. Rev. Lett. **91**, 158302 (2003).
[6] C. Storm, J. J. Pastore, F. C. MacKintosh, T. C. Lubensky, and P. A. Janmey, Nature (London) **435**, 191 (2005).
[7] A. M. Stein, D. A. Vader, D. A. Weitz, and L. M. Sander, Complexity **16**, 22 (2011).
[8] D. Weaire and S. Hutzler, Philos. Mag. **83**, 2747 (2003).
[9] B. P. Tighe, Granular Matter (2013), doi: 10.1007/s10035-013-0436-6.
[10] S.-G. Baek and J. J. Magda, J. Rheol. **37**, 1201 (1993).
[11] V. G. Kolli, E. J. Pollauf, and F. Gadala-Maria, J. Rheol. **46**, 321 (2002).
[12] A. Singh and P. R. Nott, J. Fluid Mech. **490**, 293 (2003).
[13] A. Montesi, A. A. Peña, and M. Pasquali, Phys. Rev. Lett. **92**, 058303 (2004).
[14] M. Moan, T. Aubry, and F. Bossard, J. Rheol. **47**, 1493 (2003).
[15] J. F. Brady and I. C. Carpen, J. Non-Newton. Fluid Mech. **102**, 219 (2002).
[16] V. A. Davis, L. M. Ericson, A. N. G. Parra-Vasquez, H. Fan, Y. Wang, V. Prieto, J. A. Longoria, S. Ramesh, R. K. Saini, C. Kittrell *et al*., Macromolecules **37**, 154 (2004).
[17] S. Lin-Gibson, J. A. Pathak, E. A. Grulke, H. Wang, and E. K. Hobbie, Phys. Rev. Lett. **92**, 048302 (2004).
[18] S. B. Kharchenko, J. F. Douglas, J. Obrzut, E. A. Grulke, and K. B. Migler, Nat. Mater. **3**, 564 (2004).
[19] Z. G. Nicolaou and A. E. Motter, Nat. Mater. **11**, 608 (2012).
[20] R. Lakes, Science **235**, 1038 (1987).
[21] R. H. Baughman, J. M. Shacklette, A. A. Zakhidov, and S. Stafstrom, Nature (London) **392**, 362 (1998).
[22] P. A. Janmey, M. E. McCormick, S. Rammensee, J. L. Leight, P. C. Georges, and F. C. MacKintosh, Nat. Mater. **6**, 48 (2007).
[23] E. Conti and F. C. MacKintosh, Phys. Rev. Lett. **102**, 088102 (2009).
[24] H. Kang, Q. Wen, P. A. Janmey, J. X. Tang, E. Conti, and F. C. MacKintosh, J. Phys. Chem. B **113**, 3799 (2009).
[25] J. Wilhelm and E. Frey, Phys. Rev. Lett. **91**, 108103 (2003).
[26] L. D. Landau and E. Lifshitz, *Theory of Elasticity* (Pergamon Press, New York, 1986).
[27] E. M. Huisman, C. Storm, and G. T. Barkema, Phys. Rev. E **82**, 061902 (2010).
[28] E. M. Huisman, C. Storm, and G. T. Barkema, Phys. Rev. E **78**, 051801 (2008).
[29] M. Rubinstein and R. H. Colby, *Polymer Physics* (Oxford University Press, New York, 2007).
[30] C. Storm and P. C. Nelson, Phys. Rev. E **67**, 051906 (2003).
[31] J. R. Shewchuk, "An Introduction to the Conjugate Gradient Method Without the Agonizing Pain," http://cs.cmu.edu/∼quake-papers/painless-conjugate-gradient.pdf.